Modeling the atomic structure of amorphous steels using crystalline approximants

V. Yu. Kazimirov,[1] Despina Louca,[1,*] V. Ponnambalam,[1] S. J. Poon,[1] and T. Proffen[2]
[1]*University of Virginia, Department of Physics, Charlottesville, Virginia 22904, USA*
[2]*Los Alamos National Laboratory, Los Alamos, New Mexico 87545, USA*
(Received 2 February 2005; revised manuscript received 14 June 2005; published 18 August 2005)

Using the pair density function analysis of pulsed neutron diffraction data, the local topology of Fe-based metallic glasses with good glass forming ability was investigated upon alloying with transition metal ions of Y, Zr, or Mo. Distinct short and medium range atomic order with common characteristics in all the glasses is observed. The local order is well described by a geometrical model constructed from superposition of "crystalline approximant" phases which is different from Frank-Kasper polyhedra clustering or dense random packing models. The mechanism responsible for the structure in the glass phase might involve a frustration-induced structural disorder of the crystalline approximant phases as they are driven away from stable stoichiometric compositions.

DOI: 10.1103/PhysRevB.72.054207 PACS number(s): 61.43.Dq, 61.12.−q, 71.55.Jv, 81.05.Kf

The mechanism that leads to glass formation or vitrification is still not well understood even for ordinary silicate glasses. This is even more so in metallic glass systems due to the complex nature of the metallic bonding where it is necessary to account for the interatomic interactions by considering strong electron correlation effects. Recent advances in metallic glass preparation have renewed the interest in this class of materials because they can be prepared in bulk form (several millimeters in diameter), with yield strengths higher than stainless steel, high elastic moduli, and without using expensive noble metals.[1,2] Several empirical rules have been implemented over the years as guidelines for glass preparation with some success particularly in the Zr [i.e., Zr—Al-(Ni or Cu)] and Al [i.e., Al—Fe-(Si or Ge)] based alloys. These include a large negative heat of mixing of the constituent elements, and mixing of at least three chemically different species with a greater than 10% difference in their atomic radii.[3] Although concepts for the driving mechanism such as the atomic size factor have been proposed,[4,5] theoretical predictions of glasses have not caught up with the discovery of systems in the laboratory. A better understanding of the glassy phase may be achieved if the true nature of one of the factors believed to be important in the glass forming ability, the amorphous atomic structure, is resolved. The approach used in the present study is distinctly different from other attempts to describe the structure of amorphous alloys as we consider the amorphous state to result from competing interactions among nearby equilibrium crystalline phases present in the phase diagram.

Whether or not a liquid can be stabilized to form a glass against the precipitation of crystalline phases depends on three factors that include thermodynamic, kinetic, and structural considerations.[6] The balance among these three factors is especially important in metallic glasses because atoms interact via nearly isotropic potentials that can easily drive the system to solidify to a crystalline ground state.[7] In this paper, we focus on the structural aspects by presenting neutron scattering results on alloys with varying ion size and composition and with varying magnitude of the diameter of the glass forming alloys, i.e., ribbons versus rods. Glasses with strong glass forming ability exhibit well-defined short and medium-range order (SMRO) in their atomic topology as shown in several systems.[8] Glass stability appears to be in part determined by the presence of SMRO which becomes an important criterion for glass formation.[9] It has also been suggested that signatures of glass fragility can be frozen into the glass structure and can be represented by features such as the sharpness of structural peaks[10] or the presence or absence of the first diffraction peak. For this reason, the origin of the resulting SMRO needs to be understood.

An approach to modeling the SMRO involves the close packing of Frank-Kasper coordination polyhedra with 12 coordinated environments.[11,12] Icosahedral packing is favored in metallic glasses both from the energetics and packing point of view. Their presence is considered to stabilize a glass against crystallization[7] and has recently been alluded in undercooled melts of $Ti_{39.5}Zr_{39.5}Ni_{21}$.[13] Existence of icosahedral packing has also been suggested in Fe—B metal-metalloid alloys,[14] the metallic glasses of interested in this work. Another approach to modeling the atomic structure involves the construction of simple geometrical models composed of dense random packing of hard spheres (DRP),[15] subsequently leading to the development of more physically well-founded molecular dynamics and first principles (*ab initio*) calculations.[16] More recently it was suggested that instead of hard spheres, the use of ellipsoids would lead to more stable and efficient packing.[17] A third approach proposed theoretically for binary models but never tested on metallic glasses with three components involves the destabilization of crystalline phases where the glass phase evolves through frustration of local shear deformations within competing crystalline states.[18] In this scenario, common features in the glass and crystalline structures might be observed in a manner very similar to martensitic transformations. In general, strong glass formers have often been associated with a strong tendency for SMRO formation[19] and its characterization can be a first step to understanding stability in metallic alloys.

Pulsed neutron scattering was used to investigate three alloys at optimal concentrations, $Fe_{75}Y_5B_{20}$ (F—Y—B), $Fe_{64}Mo_{14}(CB)_{22}$ (F—Mo—C—B), and $Fe_{68}Zr_{10}B_{22}$

(F—Z—B), either in bulk metallic glass form or precursors to forming bulk metallic glasses.[20] The selected alloys exhibit high yield strengths, with sometimes plastic behavior and magnetic transitions well below room temperature.[20,21] Using the pair density function (PDF) analysis to determine their local atomic topology, we found that alloying with Mo, Zr, or Y yields three different Fe—B structural glasses[2] with similar atomic characteristics that can be described well using a simple model. Differences in their local structures can be understood in terms of their different ionic sizes and local volumes that modify the interactions between the ions. It is shown that their local amorphous structures closely resembles that of neighboring crystalline phases. Their local environment is best represented by hybrid models built from a combination of crystalline approximants of $Fe_{23}B_6$ ($Fm\bar{3}m$, $Cr_{23}C_6$ structure), $Fe_{14}TM_2B$ ($P4_2/mmm$), and $Fe_{62}TM_3B_{14}$ ($Im\bar{3}m$) (TM—transition metal). The transition to the glass structure occurs through local frustration as the competing crystalline phases are destabilized when they are driven out of their stoichiometric range.

Alloys were synthesized following the procedures described elsewhere.[20] Amorphous ribbons of F—Y—B and F—Z—B were fabricated using the melt spinning technique. Amorphous rods of F—Mo—C—B were fabricated in argon atmosphere by the copper mold casting technique. The neutron diffraction data for F—Mo—C—B, F—Z—B were collected at room temperature using the special environment powder diffractometer of the Intense Pulsed Neutron Source (IPNS) and data for F—Y—B were collected at the neutron powder diffractometer at the Los Alamos Neutron Science Center (LANSCE). Data were collected over long periods of time (about 15 h/sample) to ensure good counting statistics and to compensate for the high neutron absorption cross section of boron. The total $S(Q)$, corrected for instrumental background, absorption, incoherent, multiple, and inelastic scattering, was Fourier transformed to obtain the PDF. The PDF provides a real-space representation of atomic pair correlations and it is ideal for the analysis of amorphous systems. Details of this technique can be found in Refs. 22 and 23.

The PDFs deduced from the diffraction data of the three alloys are shown in Fig. 1. The data are plotted up to 7 Å for clarity. In F—Mo—C—B (dotted line), the first peak corresponds to the shortest bond length in the structure and is due to Fe—B/C and Mo—B/C pair correlations. Following is the strongest peak in the PDF corresponding to predominantly Fe—Fe correlations because the concentration of Fe is the highest, and Fe has the largest neutron cross section of all the constituent elements. The mean Fe—Fe bond length obtained at the full width half maximum (FWHM) of the peak is ~2.52 Å and is slightly longer than the nominal Fe—Fe bond length of 2.48 Å assuming metallic bonding as in pure Fe metal. To the right of this peak, Fe—Mo and Mo—Mo pairs contribute to the intensity of the peak. Beyond this coordination sphere, second and third order correlations between pairs become less well defined because of the increasing structural randomness and bond length distribution from different kinds of atom pairs. This is typical of amorphous alloys where long-range order is absent. The local structure features observed in this metallic glass alloy are characteristic of the other two metallic glasses studied, F—Y—B and F—Z—B, and are shown in the figure as well. However, the different bonding schemes between Y, Zr, and Mo and the corresponding variations in their properties (i.e., Y and Zr are in ribbon form while Mo can be prepared in rod form) manifest in important subtle ways that can be seen in the structural details. In particular, in the case of the Mo alloy, a small first diffraction peak which serves as a signature of medium range ordering[24,25] is observed in the structure function (see inset in Fig. 1) but not in the Zr and Y alloys. The presence of this diffraction peak is important as it provides a connection to the structure in the liquid state.[26] In real space, the position and shape of several PDF peaks are different from alloy to alloy because the TM ion size changes from one alloy to the other and this has important consequences on the local volume. As the nominal atomic radius increases from Mo (1.36 Å) to Zr (1.59 Å) to Y (1.78 Å) (Ref. 27) noticeable differences are observed in the first peak and in the structure beyond 2.8 Å. As the Mo ion is nominally the smallest of the three, the first peak shifts to the left while with the larger Y ion, the peaks shift to the right. Zr peaks are intermediate to those of Y and Mo. Thus the shift of the PDF peaks to higher r values can be explained in terms of the increasing TM size which changes the local volume and local interactions among the ions.[28] This could directly affect the magnetic exchange interactions and the ferromagnetic transition temperature. Note that with Y, the largest ion, the amount necessary to achieve glass formation is a third of that needed with the smallest ion, Mo. This might be because the large size of Y creates a nucleation source for distortion that propagates over longer distances.

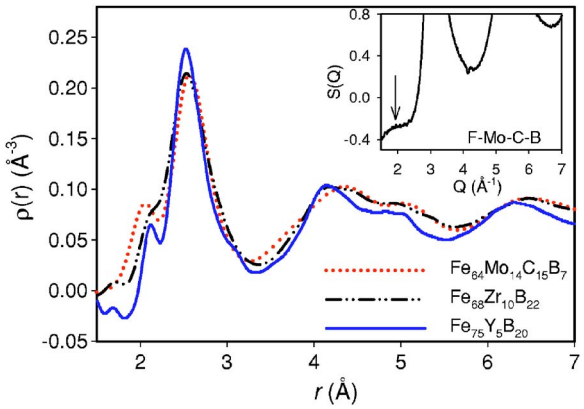

FIG. 1. (Color online) A plot of the experimentally determined PDFs corresponding to the local atomic structures for $Fe_{64}Mo_{14}(CB)_{22}$, $Fe_{68}Zr_{10}B_{22}$ and $Fe_{75}Y_5B_{20}$ alloys.

To determine the local ordering that reproduces the SMRO observed in the three alloys, crystalline approximants were used to construct a three-dimensional atomistic model. One of these compounds is the metastable $Fe_{23}B_6$ that forms upon devitrification of F—Mo—C—B (See Ref. 2) and F-Y-B.[29] In Fig. 2 (top), a model for the local structure for $Fe_{23}B_6$ is shown, calculated from $\rho(r) = (1/4\pi Nr^2)\Sigma_{i,j}(b_i b_j/\langle b\rangle^2)\delta(r-r_{ij})$ (See Ref. 30) assuming as input the atomic coordinates and unit cell dimensions from

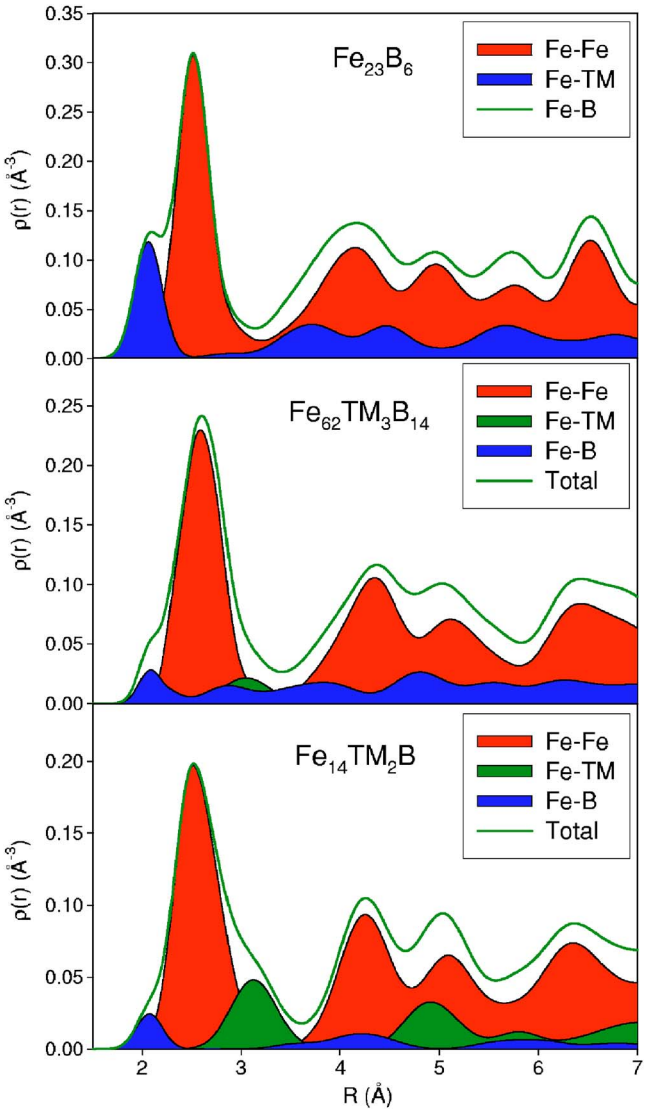

FIG. 2. (Color online) Plots of the calculated PDFs of the crystalline approximant phases used in the modeling: (a) $Fe_{23}B_6$, (b) $Fe_{14}TM_2B$, and (c) $Fe_{62}TM_3B_{14}$. Also shown are partial functions of pairs of atoms with significant contributions.

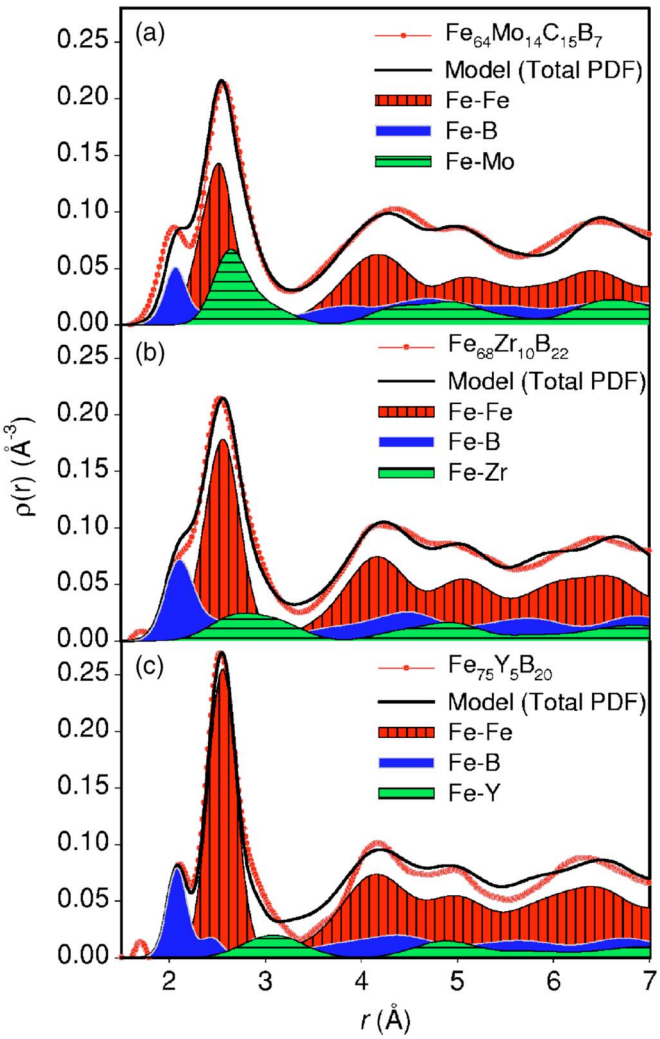

FIG. 3. (Color online) Comparison of the experimentally determined PDFs of the three alloys to the corresponding hybrid models provides strong evidence for topological SRO in Fe metallic glasses that closely resembles the metastable phases. Also shown are partial functions for selected pairs of atoms to indicate their contributions in real space. The agreement factors and packing fractions are listed in Table I.

Ref. 31. Also shown are partial functions of correlations with significant contributions. To a first approximation, its local symmetry resembles that of the Fe amorphous alloys and provides an adequate description of the SRO up to ~3 Å as seen by comparing this model to the PDFs of Fig. 1. In particular, the short-range correlations of Fe—B and Fe—Fe are directly reproduced by this model but it cannot account for the TM correlations.

The model is further improved by adding a second crystalline approximant phase that can be one of two compounds, $Fe_{62}TM_3B_{14}$ and $Fe_{14}TM_2B$ (also shown in Fig. 2), with coordinates obtained from Refs. 32–34. Differences in the local topology between these two crystalline compounds lie in the TM and Fe—B contribution as seen from the partial functions. In the case of the former compound, the Fe—B contribution (blue color) is spread throughout space and the Fe-TM contribution (green color) is visible mostly around 3 Å, while in the latter compound, the Fe—B contribution is weak (due to small concentration of B in this compound) while the Fe-TM contribution is strong. The addition of one of these phases is necessary because $Fe_{23}B_6$ alone cannot provide an adequate representation of the TM correlations, and combined, they form possible crystalline precursor structures to the glass phase as seen below. Other compounds such as Fe_2B and Fe_3B binary alloys were used in the modeling but the agreement with the experimental data was poor.

The local atomic hybrid model resulting from the superposition of $Fe_{23}B_6$ with one of the two phases provides a very good representation of the atomic correlations observed experimentally for the three alloys. The short and medium range order of the Fe—B glasses is described quite well by such geometrical model as seen by directly comparing the hybrid structures to the experimentally determined PDFs (Fig. 3). In (a), the SMRO in F—Mo—C—B alloy is best described by a hybrid structure made of $Fe_{23}B_6$

TABLE I. A list of model parameters for $Fe_{64}Mo_{14}(CB)_{22}$, $Fe_{68}Zr_{10}B_{22}$, and $Fe_{75}Y_5B_{20}$. The agreement factor is calculated using $A^2=\int[\rho_{exp}(r)-\rho_{mod}(r)]^2dr/\int\rho_0^2dr$ (See Ref. 23) and provides a measure of the goodness of fit.

Glass	Hybrid model (% phase)	Packing fraction	Agreement
$Fe_{64}Mo_{14}(CB)_{22}$	$0.2(Fe,B)_{23}B_6+0.8(Fe,Mo)_{62}Mo_3B_{14}$	0.63	0.138
$Fe_{68}Zr_{10}B_{22}$	$0.55(Fe,B)_{23}B_6+0.45(Fe,Zr)_{14}Zr_2B$	0.61	0.079
$Fe_{75}Y_5B_{20}$	$0.4(Fe,B)_{23}B_6+0.6Fe_{14}Y_2B$	0.67	0.152

$+Fe_{62}Mo_3B_{14}$. In (b), the SMRO in Fe—Zr—B is compared to a model that consists of $Fe_{23}B_6+Fe_{14}Zr_2B$ phases. In (c), F-Y-B is best described by a combination of $Fe_{23}B_6$ $+Fe_{14}Y_2B$ phases. The agreement factor calculated for all three models is quite good as shown in Table I. The percent of each phase for each model is also given in Table I along with the packing fractions. It can also be seen that both F-Y-B and F-Z-B are best fit using the $Fe_{23}B_6+Fe_{14}TM_2B$ combination. This is because of the larger size of Y and Zr that require distinctly separate contributions from Fe and these are possible using the $Fe_{14}TM_2B$ compound. On the other hand, Mo is small and its contributions are not well separated from that of Fe and for this reason $Fe_{62}TM_3B_{14}$ works well. The partial functions of Fe—Fe, Fe—B and Fe-TM are also shown in all the panels of Fig. 3. One can clearly see the effects of the ionic size with regard to the position of the different correlation peaks. These have an effect on the Fe—Fe correlations and subsequently on their magnetic interactions. The representation of the SMRO with these structures is distinctly different from the Frank-Kasper polyhedra packing.[35,36] This approach suggests that the destabilization of the crystalline phases through local frustration as they are driven away from stoichiometry leads to the glass transition. The two phases are necessary as they give rise to two different local environments and the resulting structure is not a nanocrystalline phase.

The competition between vitrification and crystallization renders a very complex phase diagram with several competing phases usually appearing with cooling. Different phases can also appear depending on the cooling rate. The close proximity of glassy to crystalline regimes in the phase diagram implies that if a quasicontinuous transformation from one to the other takes place, the two regimes might exhibit similarities in their equilibrium structures. The glass structure might resemble the local topology of nearby stable or metastable crystalline phases but without the periodic constraints of the crystals due to frustration of the local interactions.

The atomic volume obtained from these models can be directly compared to the results reported by Wang *et al.*,[37] from models of the electronic and magnetic structure of Fe-based amorphous alloys (Fe—Mn—Zr—B, Fe—Mn—Mo—C—B). From simulations of the atomic structure of these compounds based on an *ab initio* Monte-Carlo technique, they obtained atomic volumes of 11.56 and 11.2 $Å^3$ for Fe—Mn—Zr—B and Fe—Mn—Mo—C—B, respectively. These values are comparable to 12.06 and 11.24 $Å^3$ for Fe—Zr—B and Fe—Mo—C—B, respectively, obtained from our models. Considering the differences in the chemical compositions between the compounds we can conclude that our results are close to the results of the *ab initio* calculations. This means that the tendency of changing atomic volumes with chemical composition was described correctly by our models.

The formulation of the local order in amorphous glasses from neighboring crystalline phases is consistent with the crystal to glass transition in binary models proposed in Ref. 18. From these results we can deduce that although locally differences are expected when different size and concentration of the solute ions are introduced in the Fe—B substructure, a very similar equilibrium state ensues because the mechanism for glass formation must be the same in the three different glasses under investigation. This mechanism might be applicable to all good glass formers and it might be because these glasses are close to eutectics as suggested in Ref. 38. While icosahedral packing has been used so far to describe the SMRO, this appears adequate for metal-metal alloys although very few direct comparisons with experiments exist in the literature. On the other hand, the crystalline approximant method appears to provide a physical description of the nature of the atomic ordering in metal-metalloid alloys. At the same time, it is understood that such a model provides insufficient understanding of the energetics of the interactions and the dynamics of the transition. Nevertheless, the approach used in the present work may be useful as these models can serve as a starting point to molecular dynamics and *ab initio* methods. Also, these models present a physical advantage compared to the DRP approach. The main principle of DRP is geometrical packing and it takes into account no real interatomic interactions. In contrast to DRP, the use of real crystalline compounds makes a good starting point and, consequently, the structure based on our model is more realistic than the abstract geometrical structures based on DRP.

The authors would like to acknowledge valuable discussions with T. Egami, M. Widom, D. Nicholson, and Y. Wang. They also thank S. Short for assistance with the SEPD measurements. Partial treatment of the experimental data was done using the PDFgetN software[39] and modeling was performed using the Lady software.[40] The work was performed under the auspices of DARPA/ONR under Grant No. N00014-01-1-0961 at the University of Virginia. The IPNS is supported by the U.S. Department of Energy under Contract No. W-31-109-Eng-38 and LANSCE is supported by the U.S. Department of Energy under Contract No. W-7405-ENG-36.

*Author to whom correspondence should be addressed. Electronic address: louca@virginia.edu

[1] W. L. Johnson, Mater. Res. Soc. Symp. Proc. **554**, 311 (1998); H. Smith, in *Rapidly Solidified Alloys: Processes, Structures, Properties, Applications*, edited by H. H. Liebermann (Dekker, New York, 1993), p. 617.

[2] V. Ponnambalam, S. J. Poon, and G. J. Shiflet, J. Mater. Res. **19**, 1320 (2004).

[3] A. Inoue, Mater. Trans., JIM **36**, 866 (1995); A. Inoue *et al.*, Mater. Res. Soc. Symp. Proc. **554**, 251 (1999).

[4] T. Egami and Y. Waseda, J. Non-Cryst. Solids **64**, 113 (1984).

[5] C. A. Angell, Science **267**, 1924 (1995).

[6] Z. P. Lu and C. T. Liu, Phys. Rev. Lett. **91**, 115505 (2003).

[7] M. Ronchetti and S. Cozzini, in *Defects and Disorder in Crystalline and Amorphous Solids*, edited by C. R. A. Catlow (Kluwer Academic, Netherlands, 1994), p. 391.

[8] H. Y. Hsieh T. Egami, Y. He, S. J. Poon, and G. J. Shiflet, J. Non-Cryst. Solids **135**, 248 (1991); K. D. Machado, J. C. de Lima, C. E. M. de Cmpos, T. A. Grandi, and D. M. Triches, Phys. Rev. B **66**, 094205 (2002); T. C. Hufnagel and S. Brennan, *ibid.* **67**, 014203 (2003).

[9] J. F. Sadoc, in *Physics of Glasses. Structure and Dynamics*, edited by P. Jund and R. Jullien, AIP Conf. Proc. No. 489 (AIP, Melville, NY, 1999), p. 105.

[10] P. S. Salmon, R. A. Martin, P. E. Mason, and G. J. Cuello, Nature (London) **435**, 75 (2005).

[11] F. C. Frank and J. S. Kasper, Acta Crystallogr. **11**, 184 (1958); F. C. Frank, Proc. R. Soc. London, Ser. A **215**, 43 (1952).

[12] S. Sachdev and D. R. Nelson, Phys. Rev. Lett. **53**, 1947 (1984).

[13] K. F. Kelton, G. W. Lee, A. K. Gangopadhyay, R. W. Hyers, T. J. Rathz, J. R. Rogers, M. B. Robin, and W. S. Robinson, Phys. Rev. Lett. **90**, 195504 (2003).

[14] E. Matsubara, S. Sato, M. Imafuku, T. Nakamura, H. Koshiba, A. Inoue, and Y. Waseda, Mater. Trans., JIM **41**, 1379 (2000).

[15] J. D. Bernal, Nature (London) **185**, 68 (1960).

[16] G. Gutierrez and B. Johansson, Phys. Rev. B **65**, 104202 (2002).

[17] A. Donev, I. Cisse, D. Sachs, E. Variano, F. H. Stillinger, R. Connelly, and S. Torquato, Science **303**, 990 (2004).

[18] M. Li and W. L. Johnson, Phys. Rev. Lett. **70**, 1120 (1993).

[19] H. Tanaka, Phys. Rev. Lett. **90**, 055701 (2003).

[20] V. Ponnambalam, S. J. Poon, G. J. Shiflet, V. M. Keppens, R. Taylor, and G. Petculescu, Appl. Phys. Lett. **83**, 1131 (2003).

[21] V. Ponnambalam, S. J. Poom, and G. J. Shiflet, J. Mater. Res. **19**, 3046 (2004).

[22] B. H. Toby and T. Egami, Acta Crystallogr., Sect. A: Found. Crystallogr. **48**, 336 (1992).

[23] D. Louca and T. Egami, Phys. Rev. B **59**, 6193 (1999).

[24] K. Ahn, D. Louca, S. J. Poon, and G. J. Shiflet, J. Phys.: Condens. Matter **15**, S2357 (2003).

[25] K. Ahn, D. Louca, S. J. Poon, and G. J. Shiflet, Phys. Rev. B **70**, 224103 (2004).

[26] D. Louca, K. Ahn, A. K. Soper, S. J. Poon, and G. J. Shiflet, in, *Amorphous and Nanocrystalline Metals*, edited by R. Busch, T. C. Hufnagel, J. Eckert, A. Inoue, W. L. Johnson, and A. R. Yavari, MRS Symposia Proceedings No. 806 (Materials Research Society, Pittsburg, 2004), p. 269.

[27] R. D. Shannon, Acta Crystallogr. **A32**, 751 (1976).

[28] The change in the peak intensity is because the PDF is normalized by the concentration of the elements and their neutron scattering lengths, b_{coh}. For Mo, Zr, and Y they are 6.72, 7.16, and 7.75 fm, respectively.

[29] T. Nakamura, H. Koshiba, M. Imafuku, A. Inoue, and E. Matsubara, Mater. Trans., JIM **43**, 1918 (2002).

[30] Since masses are considered as point charges in this model, substitution of elements with different sizes is simulated by changing the unit cell dimensions as well as refine the atomic coordinates.

[31] P. Villars and L. D. Calvert, in Pearson's Handbook on Crystallographic Data for Intermetallic Phases Vol. 2, (American Society of Metals, Metals Park, Ohio, 1985), p. 1297.

[32] D. Givord, H. S. Li, and R. P. de la Bătie, Solid State Commun. **88**, 907 (1993).

[33] L. Withanawasam, A. S. Murthy, G. C.Hadjipanayis, K. R. Lawless, and R. F. Krause, J. Magn. Magn. Mater. **140–144**, 1057 (1995).

[34] G. Bocelli, G. Calestani, A. Deriu, and F. Leccabue, Solid State Commun. **61**, 451 (1987).

[35] D. W. Qi and S. Wang, Phys. Rev. B **44**, 884 (1991).

[36] L. Hui, B. Xiufang, and W. Guanghou, Phys. Rev. B **67**, 094202 (2003).

[37] Y. Wang and M. Widon (unpublished).

[38] Z. P. Lu, C. T. Liu, J. R. Thompson, and W. D. Porter, Phys. Rev. Lett. **92**, 245503 (2004).

[39] P. F. Peterson, M. Gutmann, Th. Proffen, and S. J. L. Billinge, J. Appl. Crystallogr. **33**, 1192 (2000).

[40] M. B. Smirnov and V. Yu. Kazimirov, Comm. Joint Institute for Nuclear Research, E14-2001-159 (2001).